Cell-Free HPV DNA Provides an Accurate and Rapid Diagnosis of HPV-Associated Head and Neck Cancer

Giulia Siravegna[1,2], Connor J. O'Boyle[3], Shohreh Varmeh[3,4], Natalia Queenan[3], Alexa Michel[2], Jarrod Stein[3], Julia Thierauf[5], Peter M. Sadow[1,3,5], William C. Faquin[1,3,5], Simon K. Perry[5], Adam Z. Bard[5], Wei Wang[6], Daniel G. Deschler[1,3], Kevin S. Emerick[1,3], Mark A. Varvares[1,3], Jong C. Park[1,7], John R. Clark[1,7], Annie W. Chan[1,8], Vanessa Carlota Andreu Arasa[9], Osamu Sakai[9], Jochen Lennerz[1,2,5], Ryan B. Corcoran[1,2,7], Lori J. Wirth[1,7], Derrick T. Lin[1,3], A. John Iafrate[1,2,5], Jeremy D. Richmon[1,3], and Daniel L. Faden[1,3,10]

ABSTRACT

Purpose: HPV-associated head and neck squamous cell carcinoma (HPV+HNSCC) is the most common HPV-associated malignancy in the United States and continues to increase in incidence. Current diagnostic approaches for HPV+HNSCC rely on tissue biopsy followed by histomorphologic assessment and detection of HPV indirectly by p16 IHC. Such approaches are invasive and have variable sensitivity.

Experimental Design: We conducted a prospective observational study in 140 subjects (70 cases and 70 controls) to test the hypothesis that a noninvasive diagnostic approach for HPV+HNSCC would have improved diagnostic accuracy, lower cost, and shorter diagnostic interval compared with standard approaches. Blood was collected, processed for circulating tumor HPV DNA (ctHPVDNA), and analyzed with custom ddPCR assays for HPV genotypes 16, 18, 33, 35, and 45. Diagnostic performance, cost, and diagnostic interval were calculated for standard clinical workup and compared with a noninvasive approach using ctHPVDNA combined with cross-sectional imaging and physical examination findings.

Results: Sensitivity and specificity of ctHPVDNA for detecting HPV+HNSCC were 98.4% and 98.6%, respectively. Sensitivity and specificity of a composite noninvasive diagnostic using ctHPVDNA and imaging/physical examination were 95.1% and 98.6%, respectively. Diagnostic accuracy of this noninvasive approach was significantly higher than standard of care (Youden index 0.937 vs. 0.707, $P = 0.0006$). Costs of noninvasive diagnostic were 36% to 38% less than standard clinical workup and the median diagnostic interval was 26 days less.

Conclusions: A noninvasive diagnostic approach for HPV+HNSCC demonstrated improved accuracy, reduced cost, and a shorter time to diagnosis compared with standard clinical workup and could be a viable alternative in the future.

Introduction

Advancements in cell-free DNA (cfDNA) isolation and analytic approaches have led to the exploration and implementation of cfDNA for tumor molecular profiling, treatment monitoring, and detection of residual disease and recurrence (1, 2). In addition, significant interest is currently focused on cfDNA for cancer screening and early detection (3, 4). Use of cfDNA in the screening and diagnostic settings has been limited by ongoing challenges associated with sensitivity (detecting somatic cfDNA alterations in a background of normal DNA), and specificity (cfDNA alterations are not inherently specific to a given cancer type).

HPV-associated cancers make up 5% of all cancers worldwide. In the United States, HPV-associated oropharyngeal squamous cell carcinoma (HPV+OPSCC) is the most common HPV-associated malignancy and continues to increase in incidence (5–7). In addition to somatic cfDNA, HPV-associated cancers release circulating tumor HPV DNA (ctHPVDNA), with the added advantages that ctHPVDNA is more easily detected than altered somatic cfDNA, leading to improved sensitivity, and that ctHPVDNA is specific to the anatomic sites in which HPV-associated cancers arise, quickly narrowing site of origin, and improving specificity (8–18). Existing work has demonstrated that most patients with HPV+OSPCC have ctHPVDNA detectable in the blood at the time of first presentation by either droplet digital PCR (ddPCR) or next-generation sequencing (NGS)-based methods, and that this finding is highly specific for malignancy (13–17).

Current College of American Pathologists Clinical Practice Guidelines for diagnosing HPV+OPSCC recommend tissue sampling followed by histomorphologic examination for confirmation of SCC and testing for HPV involvement by p16 IHC, a surrogate marker for high-risk HPV infection (19). In addition to being invasive, user dependent,

[1]Harvard Medical School, Boston, Massachusetts. [2]Massachusetts General Hospital Cancer Center, Boston, Massachusetts. [3]Department of Otolaryngology-Head and Neck Surgery Massachusetts Eye and Ear, Boston, Massachusetts. [4]Medical Oncology, Dana-Farber Cancer Institute, Harvard Medical School, Boston, Massachusetts. [5]Department of Pathology, Massachusetts General Hospital, Boston, Massachusetts. [6]Departments of Medicine and Neurology, Brigham and Women's Hospital, Boston, Massachusetts. [7]Division of Hematology-Oncology, Department of Medicine, Massachusetts General Hospital, Boston, Massachusetts. [8]Department of Radiation Oncology, Massachusetts General Hospital, Boston, Massachusetts. [9]Department or Radiology, Boston Medical Center, Boston, Massachusetts. [10]Broad Institute of MIT and Harvard, Cambridge, Massachusetts.

Note: Supplementary data for this article are available at Clinical Cancer Research Online (http://clincancerres.aacrjournals.org/).

G. Siravegna and C.J. O'Boyle contributed equally to this article.

J.D. Richmon and D.L. Faden contributed equally to this article.

Corresponding Author: Daniel L. Faden, Otolaryngology-Head and Neck Surgery, Massachusetts Eye and Ear, Massachusetts General Hospital, Harvard Medical School, Broad Institute, Boston, MA 02114. E-mail: Daniel_Faden@meei.harvard.edu

Clin Cancer Res 2022;28:719–27

doi: 10.1158/1078-0432.CCR-21-3151

Translational Relevance

HPV-associated head and neck squamous cell carcinoma (HPV+HNSCC) is the most common HPV-associated malignancy in the United States and continues to increase in incidence. Current diagnostic approaches for HPV+HNSCC rely on tissue biopsy followed by histomorphologic assessment and detection of HPV indirectly by p16 IHC. Such approaches are invasive and have variable sensitivity. Here, we demonstrate that a noninvasive diagnostic approach consisting of circulating tumor HPV DNA detection combined with cross-sectional imaging and physical exam findings had higher diagnostic accuracy, reduced cost, and shorter time to diagnosis compared with standard tissue-based diagnosis. These findings provide proof of concept for an integrated noninvasive diagnostic and monitoring approach for HPV+HNSCC using circulating tumor HPV DNA.

and the high cost of procedurally-based diagnostics in general, these existing diagnostic approaches have several additional limitations (20). First, the most common diagnostic approach for biopsy of HPV+OPSCC is fine-needle aspiration (FNA) of a neck lymph node, as HPV+OPSCCs classically presents with large cystic nodal metastases and small primary tumors. In HPV+OPSCC, FNA has intrinsic failure rates of 20% to 30% due to inadequate cellular material (21–25). Further, interpretation of p16 IHC on FNA specimens lacks consensus and is variable across pathologists and institutions, leading to decreased sensitivity compared with tissue-based p16 IHC interpretation (21–25). Subsequent "open" tissue biopsy is thus often required to confirm a diagnosis of HPV+OPSCC, leading to increased costs, delays in diagnosis, multiple invasive procedures, and increased diagnostic uncertainty. Second, p16 IHC performance as a surrogate marker for HPV-associated cancer is dependent on the fraction of HPV-associated malignancies in the test population. Thus, although p16 IHC may have adequate sensitivity in a population with high rates of HPV+OPSCC, such as tissue biopsies from oropharynx tumors in the United States, performance drops significantly when applied in other clinical settings. For example, the percentage of OPSCC caused by HPV is significantly less in many other parts of the world, limiting the utility of p16 IHC in these regions. Similarly, HPV is an oncogenic driver in additional subtypes of head and neck squamous cell carcinoma (HNSCC) such as a subset of nasopharyngeal SCCs, sinonasal SCCs, and a small percentage of oral cavity SCCs (26, 27). In these low prevalence settings, p16 has significantly decreased diagnostic accuracy, for similar reasons.

Considering the diagnostic challenges associated with HPV+HNSCC and the performance of ctHPVDNA detection in the treatment and monitoring setting, we conducted a prospective observational study evaluating a ctHPVDNA-based diagnostic approach for HPV+HNSCC compared with standard clinical workup. We tested the hypothesis that a combinatorial noninvasive approach using ctHPVDNA and cross-sectional imaging/physical exam would have improved diagnostic accuracy, lower cost, and decreased time to diagnosis compared with existing approaches.

Materials and Methods

Study design and enrollment

All patients enrolled underwent written informed consent to a protocol approved by the Dana Farber/Harvard Cancer Center Institutional Review Board. The study was conducted in accordance with the U.S. Common Rule. Eligibility for inclusion were: (i) >18 years old and (ii) willing to contribute blood samples for research purposes and provide informed consent. Cases: Patients with the new or suspected diagnosis of untreated OPSCC, NPC, or SNSCC were prospectively identified upon presentation to the head and neck surgical oncology clinic at Massachusetts Eye and Ear and consecutively enrolled. All patients underwent standard of care diagnostic workup. Controls: Patients with new or suspected diagnosis of untreated OPSCC, NPC, or SNSCC who were subsequently diagnosed with HPV-negative HNSCC were used as controls (p16 IHC negative with or without direct HPV testing). Additional patients were enrolled to match cases 1:1 from the Head and Neck Surgical Oncology clinic. Controls were recruited in a 2:1 fashion, HPV-negative HNSCC controls ($n = 45$) to noncancer controls ($n = 25$; total controls, $n = 70$). All blood samples were assigned a study ID and blinded for further analysis.

HPV diagnostics

All patients with cancer underwent histomorphology assessment and p16 IHC for determination of HPV status. For p16 IHC-positive cases who did not undergo clinical direct HPV testing with HPV DNA PCR or RNA *in situ* hybridization (ISH), archived tissue was retrieved, and HPV DNA PCR was performed. Patients without direct HPV testing performed clinically and who lacked tissue for subsequent testing were excluded from the final analysis. p16 IHC and HPV test metrics can be found in Supplementary Table S1 (19, 28).

Blood collection, processing, and ddPCR

Ten to twenty milliliters of blood was collected in DNA BCT tubes (Streck) at presentation. Blood was double spun at room temperature for 10 minutes at 1,600 × *g* and then 3,000 × *g* and frozen down at −80°C until extraction. Total cfDNA was extracted from 5 mL of plasma using the QIAamp Circulating Nucleic Acid Kit (Qiagen) and quantified with a Qubit fluorometer (Thermo Fisher Scientific). ddPCR was performed on a QX-200 platform (Bio-Rad) and analyzed using QuantaSoft software v1.7.4.0917 (Bio-Rad). DNA template was added to 12.5 μL of ddPCR Supermix for Probes (Bio-Rad) and 1.25 μL of the HPV + FGFR1 primer/probe mixture.

Probes to conserved regions of HPV E7 for HPV 16, 18, 33, 35, and 45 were designed, tested, and optimized using synthetic DNA fragments (all), cell lines (16/18), and human cervical samples (33/35) based on Fractional Abundance of the HPV DNA alleles versus the DNA control probe FGFR1 in the nonviral/normal background. Samples were run at 5 to 10 ng cfDNA input and up or down titrated to optimize ddPCR performance, with a range of 1 to 20 ng of total cfDNA loaded per well. This reaction mix was added to a DG8 cartridge together with 60 μL of Droplet Generation Oil for Probes (Bio-Rad) and used for droplet generation. Droplets were then transferred to a 96-well plate (Eppendorf) and thermal cycled with the following conditions: 5 minutes at 95°C, 40 cycles of 94°C for 30 seconds, 55°C for 1 minute followed by 98°C for 10 minutes (Ramp Rate 2°C/sec). Droplets were analyzed with the QX200 Droplet Reader (Bio-Rad) for fluorescent measurement of FAM and HEX probes. Gating was performed on the basis of positive and negative controls, and HPV positive populations were identified.

HPV 16 probes were run first and if negative, HPV 33, 35, 45, and 18 were run subsequently. HPV read count results were expressed in copies/mL, which was calculated with: (copies per well)/(μL input of sample) × (μL DNA extracted/mL processed plasma). Quantification of the target molecule was presented as the number of total copies

(HPV plus FGFR1) per sample in each reaction. ddPCR analysis of normal control DNA from donor plasma and no DNA template controls were included in all runs. All samples were run at least in duplicate and cut offs for adequate sample and positive/negative were pre-emptively set at 500 FGFR1 events total and ≥2 HPV reads total and prospectively applied. In samples with 1 HPV read, when additional plasma was available, the sample was retested. Amplicon sequences are available in Supplementary Table S2.

Cost modeling

To calculate cost estimates we first designed three clinical workflows: (i) current practice (Supplementary Fig. S1A), (ii) a "realistic" liquid biopsy workflow (Supplementary Fig. S1B), and (iii) a "ideal" liquid biopsy workflow (Supplementary Fig. S1C). Estimates for modeling and decision trees were based on patients accrued to this study and practice patterns at the institution of record. Decision trees were first created by the senior author based on data from the 70 cases accrued to the trial and then reviewed and modified by two additional clinicians to ensure accuracy. The proposed diagnostic pathways entailed relevant diagnostic medical procedures from initial presentation to treatment initiation (i.e., therapeutic cost was excluded). Pathway 1A (current practice) assumes that 100% of patients are diagnosed using standard tissue sampling. Pathway 1C (ideal liquid biopsy scenario) assumes ctHPVDNA testing in all patients with ctHPVDNA testing becoming available at the specialist (General Otolaryngologist or General Medical Oncologist) level. Pathway 1B (realistic liquid biopsy pathway) assumes ctHPVDNA is available only at the subspecialist level (tertiary cancer center). Using these estimates, 10% of patients undergo tissue biopsy in the operating room for reasons of tumor localization or surgical planning in the ideal scenario versus 53.5% in the standard of care model.

We identified the specific dollar amounts [Centers for Medicare and Medicaid Services (CMS) fee schedules] by linking each dollar amount to the appropriate current procedural terminology code (CPT; American Medical Association). A complete list of CPT codes and CMS prices (Q1 2021) is provided in Supplementary Tables S3A–S3F. On the basis of the diagnostic modality pathways we created probability trees where each medical procedure is represented by a branching point with an associated probability. Each branching point's probability is conditional on the prior branch, such that the sum of probabilities of all branches at any branching point is 1. For each path through the probability tree, we calculated two numbers: the total path probability and the total procedural cost. Along paths, probabilities were multiplied, and costs were added. The expected cost of a model was calculating by adding the product of probabilities and costs across all paths.

Cross-sectional imaging scores and combined modeling

Clinically available pretreatment cross-sectional imaging was downloaded, de-identified, and coded for all cases and HPV negative HNSCC controls. Additional images from HPV negative control patients treated at the same institution presenting within the same timeframe were used to replace noncancer controls ($n = 25$). Blinded images were reviewed by two independent neuroradiologists (OS, CA) and scored on existing features known to relate to HPV+HNSCC (Supplementary Table S4; refs. 29–34). Discrepancies were resolved by discussion between the neuroradiologists.

Hypothesis and statistical analysis

The primary objective of this study was to test the hypothesis that a noninvasive ctHPVDNA liquid biopsy would be more sensitive, specific, less costly, and have decreased time to diagnosis compared with standard clinical workup. Statistical significance was assessed using a two-tailed log-rank test. Wilcoxon rank sum tests were used to compare between groups. Youden indexes were compared as described by Chen and colleagues (35).

Results

Assay characteristics

Five ddPCR assays were developed and optimized to detect conserved regions of E7 from HPV 16,18, 33, 35, and 45 (target regions 71 to 80 base pairs, Supplementary Table S2). Probes were confirmed to have no cross-genotype reactivity (Supplementary Table S5), to be linear with $R^2 > 0.96$ for all genotypes and limits of detection to ≤0.1% fractional abundance and ≤0.01 ng total concentration, equivalent to single molecule detection (Supplementary Figs. S2 and S3; Supplementary Table S6).

Patient characteristics

From January 21, 2020 to March 30, 2021, excluding a 4-month block of time due to cessation of research for the coronavirus pandemic, 70 consecutive cases and 70 controls were prospectively enrolled (**Fig. 1**). All cases had HPV+HNSCC tumors as defined by histomorphology consistent with squamous cell carcinoma, p16 IHC positivity in accordance with College of American Pathology guidelines and direct HPV confirmatory testing (Supplementary Table S1). Nine cases were excluded from the final analysis as they either lacked direct HPV testing and did not have tissue available for *post hoc* testing ($n = 6$) or because they underwent partial treatment prior to presentation ($n = 3$), leaving 61 cases for final analysis. Of note, all nine cases had detectable ctHPVDNA at presentation. 57 of 61 cases were OPSCC, 2 were nasopharyngeal SCC, 1 was sinonasal SCC, and 1 was oral cavity SCC. Cases represented the typical spectrum of patients presenting to a tertiary care cancer center for the new diagnosis of HPV+HNSCC with 46 of 61 (75%) of patients having stage 1 HPV+OPSCC (i.e., low disease burden; **Table 1**).

Clinical diagnostic workup

Clinical approaches for diagnosis were prospectively recorded for each case (**Table 2**). Similar to published work nationwide, FNA was the most common first diagnostic approach (61%, 37/61 cases). The diagnostic success rate of p16 IHC on FNA was 46% (17/37) when accounting for all cases (including those with inadequate specimen to perform the test) and 61% when including only cases with adequate sample for testing. At our tertiary care cancer center, 35% (13/37) of patients also underwent direct HPV testing on FNA which led to a diagnosis in four additional patients, yielding an overall diagnostic success rate of 57% (21/37) on FNA. 39% (24/61) of patients underwent tissue biopsy of the primary tumor as first diagnostic attempt. The overall diagnostic success rate on first attempt (FNA + primary tissue biopsy) was 72%, requiring 28% (17/61) of patients to undergo a second biopsy to achieve diagnosis.

ctHPVDNA at diagnosis

Mean ctHPVDNA at presentation was 2,675 copies/mL, median was 114 and the range was 0 to 38,670 (**Fig. 2**; Supplementary Fig. S4A). 1 of 61 cases were negative (false negative) for ctHPVDNA (Stage 1, T1 N1 M0 HPV+OPSCC). One HPV read was present in this sample, falling below the predetermined threshold of ≥2 HPV reads. No additional sample was available for testing due to low volume of blood collected. T stage and N stage were associated with ctHPVDNA

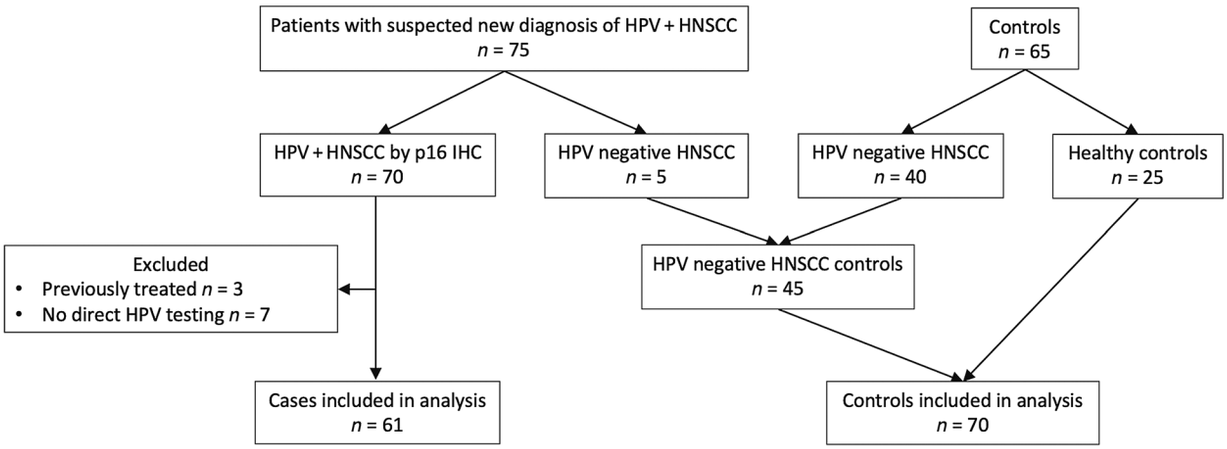

Figure 1.
CONSORT flow diagram.

levels at presentation ($P = 0.0102$ and 0.0145) whereas tumor anatomic site was not ($P = 0.62$; Supplementary Figs. S4B and S4C). 1/70 controls were positive for ctHPVDNA (false positive). This false positive was a 66-year-old male with a history of p16 negative OPSCC presenting for the first time to our center with concern for recurrent disease. ctHPVDNA was positive for HPV genotype 16. HPV16 RNA ISH was performed on the tissue block from the patient's original biopsy done at an outside institution, which was negative, coinciding with the negative p16 IHC. Repeat ctHPVDNA testing 1 month later was negative. Overall test sensitivity was 98.4%, specificity was 98.6%, positive predicative value (PPV) was 98.4%, and negative predicative value (NPV) was 98.6% (Supplementary Fig. S5A). We then compared the composite performance of standard clinical workup on first diagnostic attempt to ctHPVDNA on first diagnostic attempt. ctHPVDNA had improved diagnostic accuracy compared with standard clinical work (Youden index 0.968 vs. 0.707, $P < 0.0001$).

Table 1. Patient characteristics.

Characteristic	HPV+ HNSCC ($n = 61$)	Controls ($n = 70$)
Mean age, years (range)	62 (44–84)	54 (21–89)
Sex		
Male	52	32
Female	9	38
Race		
White	61	
TNM status		
T		
1	32	
2	24	
3	4	
4	1	
N		
0	5	
1	42	
2	10	
3	4	
M		
0	59	
1	2	
AJCC 8 staging		
1	46	
2	9	
3	6	
Tumor site		
Palatine tonsil	26	
Base of tongue	29	
Overlapping	2	
Other	4	

Noninvasive HPV+HNSCC diagnosis

We next assessed the performance of a combinatorial noninvasive approach to the diagnosis of HPV+HNSCC. To do so, we built a simple two step classifier (**Fig. 3**), which included ctHPVDNA and evidence of a mass or an enlarged lymph node in an anatomically appropriate location on cross-sectional imaging (29–34) and/or office physical exam. We applied this classifier to the blinded cases ($n = 61$), the HPV negative HNSCC controls ($n = 45$, **Fig. 1**), and 25 additional HPV negative HNSCC controls, using pretreatment cross-sectional imaging and physical exam performed as part of clinical care. 58/61 cases met criteria for diagnosis (one false negative due to ctHPVDNA and two false negatives due to lack of evidence on cross sectional imaging or physical exam). Controls remained unchanged, with one false positive patient (detectable ctHPVDNA and a mass in the pharynx). This combinatorial noninvasive diagnostic approach yielded a sensitivity of 95.1%, specificity of 98.6%, PPV of 98.3%, and NPV of 95.8% (Supplementary Fig. S5B). Restricting the analysis to only HPV+OPSCC, by far the most common HPV+HNSCC, performance metrics did not change appreciably. We then compared the composite performance of standard clinical workup on first diagnostic attempt to this combinatorial noninvasive diagnostic. Noninvasive diagnostic approach had improved diagnostic accuracy compared with standard clinical work (Youden index 0.937 vs. 0.707 $P = 0.0006$).

The high sensitivity achieved with ctHPVDNA in early stage, low tumor volume disease in this cohort, and the improved sensitivity over cross-sectional imaging and physical exam (drop in sensitivity with combined noninvasive diagnostic due to imaging/physical exam false negatives) suggests ctHPVDNA may provide improved capability for detection of ultra-low volume (subclinical) disease. Although this study was not specifically designed to assess asymptomatic disease

Table 2. Clinical diagnostic workup for HPV+HNSCC cases.

Attempt	Sample	Test	Total, *n*	Positive, *n*[a]	Diagnostic success rate
First attempt	FNA	p16	37 (28)[b]	17	46% (61%)
		DNA PCR	9	8	89%
		RNA ISH (HPV 16/18)	5	4	80%
	Tissue	p16	24	24	100%
		DNA PCR	1	1	100%
		RNA ISH (HPV 16/18)	17	16	94%
Second attempt	FNA	p16	0	0	—
		DNA PCR	0	0	—
		RNA ISH (HPV 16/18)	0	0	—
	Tissue	p16	17	17	100%
		DNA PCR	0	0	—
		RNA ISH (HPV 16/18)	14	14	100%

[a]Positive test defined as histomorphology consistent with SCC and positive HPV testing (test), in accordance with Supplementary Table S1 specifications.
[b]p16 attempted on 37 cases, 9 of which had inadequate specimen for test to be performed, leaving 28 cases for which the test performance could be evaluated. Diagnostic success was 46% using total cohort (accounting for both intrinsic and extrinsic test failures) and 61% using cases that had adequate sample for testing (accounting for intrinsic test failures only).

detection, one case encountered during this study highlights this potential. This patient was a 55-year-old male who presented to his primary care physician with a complaint of voice changes. He was then referred to an Otolaryngology clinic. Physical exam and in clinic endoscopy revealed vocal cord abnormalities, likely related to the patient's history of cigarette use. No other concerning findings were noted in upper aerodigestive track or neck (**Fig. 4A** and **B**). Because of these vocal cord findings, the patient was taken to the operating room for an examination under anesthesia and vocal cord biopsy. In accordance with standard protocol, a full examination of oral cavity, pharynx, and larynx was performed in the operating room upon which, an incidental finding of a small lesion of unclear significance in the left oropharynx was noted, in addition to the known vocal cord changes. Biopsy of this lesion was performed which demonstrated HPV+OPSCC by p16 IHC with confirmatory HPV DNA PCR for genotype 16. Vocal cord biopsy was benign. PET/CT was then performed which revealed no identifiable lesion corresponding to the biopsy proven HPV+OPSCC and no concerning neck adenopathy, clinical stage T1N0M0 HPV+OPSCC (**Fig. 4C**). The patient then underwent transoral robotic surgery and cervical lymphadenectomy with a primary tumor size on final pathology of 180 mm (3) and no involved lymph nodes, stage pT1N0M0. The patient went on to observation with no evidence of recurrent disease at the time of data analysis for this article. Blood was collected for ctHPVDNA at the time of presentation, which was positive for HPV genotype 16 (3.3 copies/mL), highlighting the sensitivity of ctHPVDNA for detection of ultra-low volume, asymptomatic disease (<200 mm^3 total tumor volume).

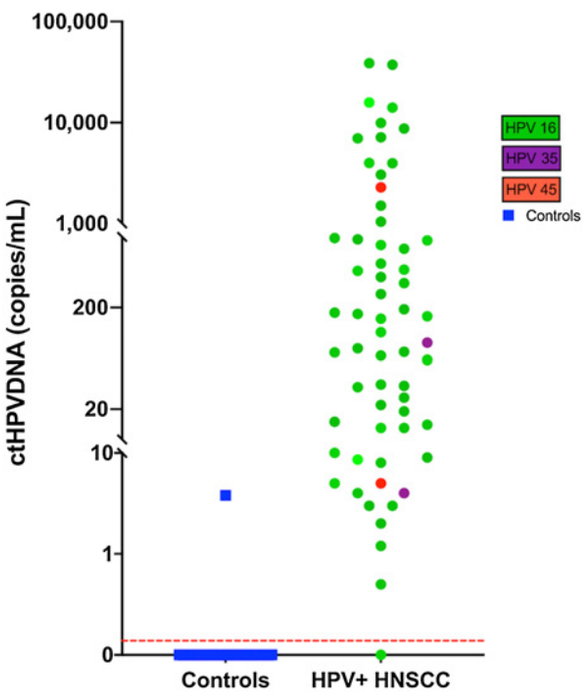

Figure 2.
ctHPVDNA at presentation. Color of circles corresponds to genotype detected. HPV status of all cases determined by direct HPV testing (RNA ISH, DNA PCR) and p16 IHC. Red dotted line represents test threshold for positive vs. negative test, demonstrating 1 case below threshold and 1 control above threshold. Green circles, HPV 16; purple circles, HPV 35; red circles, HPV 45; blue squares, controls.

Cost modeling

The average cost to achieve the diagnosis of HPV+HNSCC using modeling of standard of care pathways was $17,575. In this model, all patients undergo biopsy to achieve diagnosis and 28% undergo a second biopsy, in accordance with the patient cohort in this study (Supplementary Fig. S1A; Table 3D). Cost of diagnosis of HPV+HNSCC with ctHPVDNA replacing biopsy was modeled in two scenarios. First, we modeled a scenario in which ctHPVDNA was available only at a tertiary cancer center (sub-specialist level). Here, 33% of patients underwent tissue biopsy and 2.5% underwent a second biopsy (Supplementary Fig. S1B; Table 3F). This model estimated a cost of $11,248, 36% less than standard clinical workup (total savings per patient $6,327). Second, an ideal scenario was modeled in which ctHPVDNA was the diagnostic of choice at the specialist level and available for use. In this model 10% of patients underwent tissue biopsy and 0% underwent a second biopsy (Supplementary Fig. S1C; Table 3E). This scenario yielded a cost of $10,908, 38% less than standard clinical workup (total savings per patient $6,667).

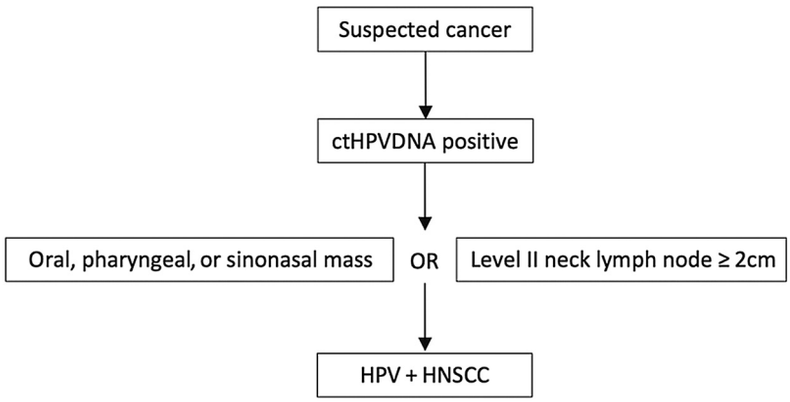

Figure 3.
Noninvasive diagnostic criteria. Oral, pharyngeal, or sinonasal mass can be detected on either cross-sectional imaging or physical examination in clinic.

Time to diagnosis

Delay in diagnoses and time to treatment impact survival outcomes in HNSCC (36, 37). To assess how a noninvasive ctHPVDNA-based approach may impact time to diagnosis, we measured the total Diagnostic Interval according to the Aarhus criteria for each case (length of time between initial clinical presentation and a final diagnosis; ref. 38). Median diagnostic interval was 41 days. We then estimated the Diagnostic Interval for a ctHPVDNA-based approach by first defining the time from first presentation to specialist visit and adding 5 days, based on existing molecular diagnostic turnaround times at our institution, and existing commercially available cfDNA assays. The median diagnostic interval for a ctHPVDNA-based approach was 15 days, a decrease of 63% (26 days).

Discussion

We have conducted a prospective observational biomarker study comparing a noninvasive diagnostic approach for HPV+HNSCC using a combination of imaging/physical exam findings and ctHPVDNA liquid biopsy to standard clinical workup with biopsy. We found that a noninvasive approach demonstrated improved diagnostic accuracy, lower cost, and shorter time to diagnosis. These findings add to an existing body of literature, which support ctHPVDNA as a highly effective biomarker of treatment response in HPV+OPSCC and highlights the potential of ctHPVDNA as a fully integrated diagnostic and monitoring approach.

ctHPVDNA was recently shown to be an accurate biomarker of treatment response following surgery and chemoradiotherapy (13, 16, 17, 39) as well as a marker of recurrence (14). This existing work also demonstrated that ctHPVDNA is detectable at the time of presentation in the majority of patients with HPV+OPSCC when using sensitive approaches such as ddPCR and NGS (13, 16, 17, 39). Therefore, we designed, tested, optimized, and validated custom ddPCR assays for HPV E7 for genotypes 16, 18, 33, 35, and 45 for the purposes of evaluating ctHPVDNA as a noninvasive diagnostic approach for all HPV+HNSCCs. Selection of genotypes and genomic regions for targeting were based on existing knowledge of the HPV genome, genotype distribution, and variation within HPV genomes. For example, the vast majority of HPV+OPSCC is caused by HPV genotype 16 (~87%). Several other genotypes are also found with relative frequency including 35, 33, and 18 (40, 41). The genotype distribution of HPV in other head and neck subsites is less well understood; however, HPV 45 appears to constitute a small but significant proportion of cases in the sinonasal tract and nasopharynx. Although variation within HPV

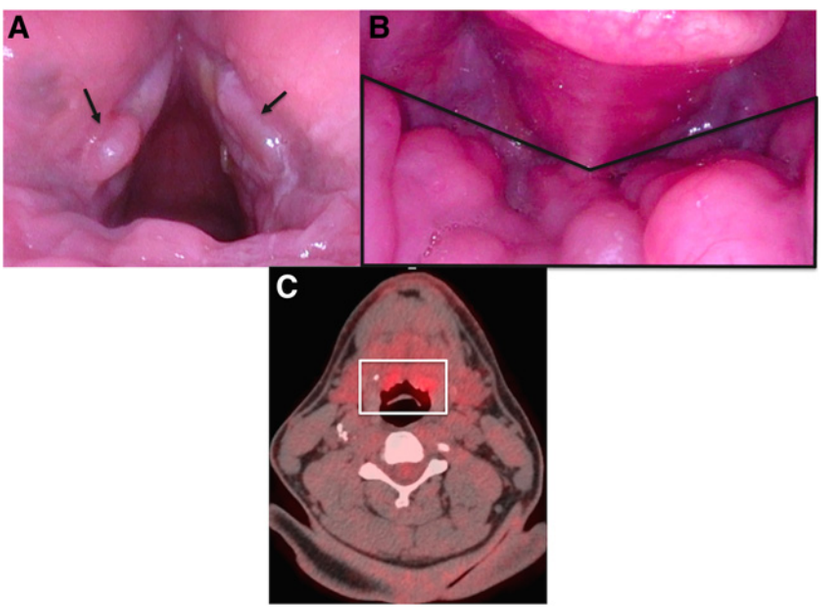

Figure 4.
Diagnostic utility of ctHPVDNA in subclinical HPV+OPSCC. **A,** In-clinic indirect laryngoscopy image of bilateral vocal cord lesions (black arrows) leading to presenting complaint. **B,** In-clinic indirect laryngoscopy image of oropharynx [black pentagon around lingual tonsils (base of tongue)] demonstrating no visible tumor on initial presentation. **C,** PET/CT demonstrating no visible tumor in the oropharynx (white box around base of tongue) after tumor had been incidentally identified on direct laryngoscopy and biopsy in operating room.

genotypes is present, for example, HPV 16 can be subcategorized at the lineage, sublineage, and SNP level, HPV E7 is highly conserved, leading to our choice for targeting E7 (42). As such, optimization studies demonstrated limits of detection down to the range of single HPV DNA fragments (Supplementary Table S6) for each genotype.

Utilizing this approach, ctHPVDNA had outstanding sensitivity and specificity (>98%) at the time of diagnosis with HPV+HNSCC. We restricted our analysis to cases which had direct HPV testing in addition to p16 IHC, to rule out potential for false positive cases. When including cases which were removed due to not having direct HPV testing or having undergone partial treatment prior to presentation, sensitivity of the assay for the total cohort ($n = 70$) was 99%, with the single false negative case having detectable ctHPVDNA but falling below the preset test threshold. Utilizing patient specific data for the cases enrolled in this study, we calculated diagnostic success of standard clinical workup for each patient finding that overall, 28% of patients required a second biopsy to achieve diagnosis. This is in line with national data which show FNA to be the most common approach and that FNA has high failure rates due to both test intrinsic and test extrinsic factors (21–25). Comparison of ctHPVDNA to standard clinical workup demonstrated a significant advantage for ctHPVDNA (Youden index 0.968 vs. 0.707, $P < 0.0001$).

Because the diagnosis of HPV+HNSCC equates to eventual treatment of that cancer, a stand-alone liquid biopsy diagnostic would likely require 100% specificity (false positives would not be tolerated). HPV+HNSCCs frequently have physical exam and imaging findings highly suggestive of the diagnosis. Therefore, we evaluated the possibility of utilizing physical exam and cross-sectional imaging findings in combination with ctHPVDNA to ensure rigor of specificity. To do so, we collected findings from the physical exam performed at first encounter with a subspecialist and cross-sectional imaging scans contained as part of clinical care for all cases enrolled and matched controls. Imaging was coded and then reviewed and graded on features previously shown to predict HPV+HNSCC by two independent head and neck neuroradiologists (29–34). Utilizing a simple metric of either a mass in an anatomic region in which HPV+HNSCCs occur or a pathologically enlarged lymph node in the appropriate level of the neck, combined with a positive ctHPVDNA level, we found that a combinatorial noninvasive diagnostic maintained excellent diagnostic accuracy while serving to increase confidence in a non-tissue-based diagnosis. This combinatorial noninvasive diagnostic would thus be closer to evolving treatment paradigms at some high volumes centers, in which FNA of a lymph node with a result of p16+ SCC combined with imaging/physical exam findings of a mass in the oropharynx is considered sufficient for treatment initiation.

Cost and time to diagnosis also favored a noninvasive approach. We found a decrease in cost of >$6,000 per patient if liquid biopsy were to replace tissue biopsy. This decrease in cost was driven largely by the costs of biopsies taken in the operating room, which is most frequently utilized when tumors are inaccessible for office biopsy, or when an initial FNA is nondiagnostic. In specific scenarios, examination under anesthesia with tissue biopsy in the operating room has utility separate from achieving diagnosis, such as to confirm location of a tumor for extirpative surgical planning. We estimated this to occur in 10% of cases and accounted for this scenario in the models. Time to diagnosis was also significantly reduced by an average of 26 days per patient with the use of liquid biopsy. This decrease was most related to the fact that many biopsy procedures require outpatient scheduling, which can add days or weeks to the diagnostic timeline, whereas bloodwork can most commonly be obtained same day. Importantly, time lag between presentation and treatment has been shown to be an independent predictor or survival in HNSCC (43).

Our study has several limitations. As this is an observational study, biases inherent to such studies exist, such as selection bias and information bias. Because of this, findings from this study require rigorous validation in independent prospective cohorts using the same prespecified diagnostic criteria. Because treatment of HPV+HNSCC is generally conducted at a dedicated cancer center or tertiary care center, patients often first present outside the healthcare system of record. Thus, to establish diagnostic interval, review of outside records was necessary following enrollment in this trial, which in some cases lacked detailed findings and required imputation of dates, which could introduce bias. With respect to our cost modeling, several limitations apply. The diagnostic modality pathways represent oversimplified assumptions (and probabilities). For example, the overall cost per model represents the average patient cost (per model) and not the real cost. Each model provides a theoretical average patient cost for each model. Further, cost modeling is an imperfect tool for cost estimation. We took the dollar amounts from the CMS fee-schedule; however, contractual rates differ across payors and reimbursement is more heterogeneous than assumed here. Specifically, we assumed perfect cost coverage of replacing the biopsy with a molecular test code; however, adoption of new diagnostic paradigms in a heterogeneous payor landscape can take decades. In other words, we did not account for the transition period away from the unprepared delivery system. Despite these limitations, our data indicate at least theoretical cost saving and we provide all details of our cost-modeling to enable verification by independent groups.

In summary, we evaluated the possibility of replacing standard tissue-based diagnosis for HPV+HNSCC with a noninvasive approach using a combination of a custom cfDNA liquid biopsy and cross-sectional imaging. We found that diagnostic accuracy was significantly improved compared with current diagnostic approaches and further, modeling supported a reduction in cost and time to diagnosis. These findings provide proof of concept for future studies to evaluate the potential for an integrated diagnostic and monitoring approach for HPV+HNSCC using ctHPVDNA.

Authors' Disclosures

P.M. Sadow reports grants from NIH NCI during the conduct of the study. K.S. Emerick reports personal fees from Regeneron outside the submitted work. V.C. Andreu Arasa reports nonfinancial support from GE Healthcare outside the submitted work. O. Sakai reports personal fees from Boston Imaging Core Lab and Bayer outside the submitted work. R.B. Corcoran reports personal fees from AbbVie, Asana Biosciences, Elicio, Guardant Health, Ipsen, Mirati Therapeutics, Natera, Navire, Qiagen, Syndax, Taiho, and Theonys; other support from Avidity Biosciences and Erasca; personal fees and other support from C4 Therapeutics, Cogent Biosciences, Kinnate Biopharma, Nested Therapeutics, nRichDx, Remix Therapeutics, and Revolution Medi; and grants from Novartiscines and Lilly outside the submitted work. L.J. Wirth reports personal fees from Bayer, Eli Lilly, Eisai, Exelixis, Genentech USA, Merck, Morphic Therapeutic, and PDS Biotechnology outside the submitted work. A.J. Iafrate reports personal fees from Invitae, Kinnate, Repare, Oncoclinicas Brasil, and Paige.ai outside the submitted work; in addition, A.J. Iafrate has a patent for Anchored multiplex PCR with royalties paid from Invitae. D.L. Faden reports personal fees from Focus on Boston and Noetic and grants from BMS outside the submitted work. No disclosures were reported by the other authors.

Authors' Contributions

G. Siravegna: Conceptualization, data curation, formal analysis, supervision, validation, investigation, methodology, writing–original draft, writing–review and editing. **C.J. O'Boyle:** Investigation. **S. Varmeh:** Writing–review and editing. **N. Queenan:** Writing–review and editing. **A. Michel:** Formal analysis, writing–

review and editing. **J. Stein:** Writing–review and editing. **J. Thierauf:** Investigation. **P.M. Sadow:** Writing–review and editing. **W.C. Faquin:** Writing–review and editing. **S.K. Perry:** Writing–review and editing. **A.Z. Bard:** Writing–review and editing. **W. Wang:** Formal analysis. **D.G. Deschler:** Writing–review and editing. **K.S. Emerick:** Writing–review and editing. **M.A. Varvares:** Writing–review and editing. **J.C. Park:** Writing–review and editing. **J.R. Clark:** Investigation. **A.W. Chan:** Investigation. **V.C. Andreu Arasa:** Writing–review and editing. **O. Sakai:** Writing–review and editing. **J. Lennerz:** Writing–review and editing. **R.B. Corcoran:** Writing–review and editing. **L.J. Wirth:** Writing–review and editing. **D.T. Lin:** Writing–review and editing. **A.J. Lafrate:** Writing–review and editing. **J.D. Richmon:** Writing–review and editing. **D.L. Faden:** Conceptualization, resources, data curation, formal analysis, supervision, funding acquisition, investigation, writing–original draft, project administration, writing–review and editing.

Acknowledgments

G. Siravegna was supported by the ECOR fund for Medical Discovery. R.B. Corcoran was supported by R01CA208437 NIH-NCI, P50CA127003, Dana Farber/Harvard Cancer Center SPORE in Gastrointestinal Cancer, Stand Up to Cancer Colorectal Dream Team Award, and U54CA224068 NIH/NCI.

The costs of publication of this article were defrayed in part by the payment of page charges. This article must therefore be hereby marked *advertisement* in accordance with 18 U.S.C. Section 1734 solely to indicate this fact.

Received September 12, 2021; revised October 15, 2021; accepted November 24, 2021; published first November 29, 2021.

References

1. Siravegna G, Marsoni S, Siena S, Bardelli A. Integrating liquid biopsies into the management of cancer. Nat Rev Clin Oncol 2017;14:531–48.
2. Wan JCM, Massie C, Garcia-Corbacho J, Mouliere F, Brenton JD, Caldas C, et al. Liquid biopsies come of age: towards implementation of circulating tumour DNA. Nat Rev Cancer 2017;17:223–38.
3. Klein EA, Richards D, Cohn A, Tummala M, Lapham R, Cosgrove D, et al. Clinical validation of a targeted methylation-based multi-cancer early detection test using an independent validation set. Ann Oncol 2021;32:1167–77.
4. Lennon AM, Buchanan AH, Kinde I, Warren A, Honushefsky A, Cohain AT, et al. Feasibility of blood testing combined with PET-CT to screen for cancer and guide intervention. Science 2020;369:eabb9601.
5. Division of Cancer Prevention and Control CfDCaP: Number of HPV-Associated Cancer Cases per Year, CDC 2019.
6. Tota JE, Best AF, Zumsteg ZS, Gillison ML, Rosenberg PS, Chaturvedi AK. Evolution of the oropharynx cancer epidemic in the United States: moderation of increasing incidence in younger individuals and shift in the burden to older individuals. J Clin Oncol 2019;37:1538–46.
7. Zhang Y, Fakhry C, D'Souza G. Projected association of human papillomavirus vaccination with oropharynx cancer incidence in the US, 2020–2045. JAMA Oncol 2021;7:e212907.
8. Dahlstrom KR, Li G, Hussey CS, Vo JT, Wei Q, Zhao CS, et al. Circulating human papillomavirus DNA as a marker for disease extent and recurrence among patients with oropharyngeal cancer. Cancer 2015;121:3455–64.
9. Cao H, Banh A, Kwok S, Shi X, Wu S, Krakow T, et al. Quantitation of human papillomavirus DNA in plasma of oropharyngeal carcinoma patients. Int J Radiat Oncol Biol Phys 2012;82:e351–8.
10. Ahn SM, Chan JYK, Zhang Z, Wang H, Khan Z, Bishop JA, et al. Saliva and plasma quantitative polymerase chain reaction-based detection and surveillance of human papillomavirus-related head and neck cancer. JAMA Otolaryngol Head Neck Surg 2014;140:846–54.
11. Bettegowda C, Sausen M, Leary RJ, Kinde I, Wang Y, Agrawal N, et al. Detection of circulating tumor DNA in early- and late-stage human malignancies. Sci Transl Med 2014;6:224ra24.
12. Wang Y, Springer S, Mulvey CL, Silliman N, Schaefer J, Sausen M, et al. Detection of somatic mutations and HPV in the saliva and plasma of patients with head and neck squamous cell carcinomas. Sci Transl Med 2015;7:293ra104.
13. Chera BS, Kumar S, Beaty BT, Marron D, Jefferys S, Green R, et al. Rapid clearance profile of plasma circulating tumor HPV type 16 DNA during chemoradiotherapy correlates with disease control in HPV-associated oropharyngeal cancer. Clin Cancer Res 2019;25:4682–90.
14. Chera BS, Kumar S, Shen C, Amdur R, Dagan R, Green R, et al. Plasma circulating tumor HPV DNA for the surveillance of cancer recurrence in HPV-associated oropharyngeal cancer. J Clin Oncol 2020;38:1050–8.
15. Hanna GJ, Lau CJ, Mahmood U, Supplee JG, Mogili AR, Haddad RI, et al. Salivary HPV DNA informs locoregional disease status in advanced HPV-associated oropharyngeal cancer. Oral Oncol 2019;95:120–6.
16. Hanna GJ, Sridharan V, Margalit DN, La Follette SK, Chau NG, Rabinowits G, et al. Salivary and serum HPV antibody levels before and after definitive treatment in patients with oropharyngeal squamous cell carcinoma. Cancer Biomark 2017;19:129–36.
17. Damerla RR, Lee NY, You D, Soni R, Shah R, Reyngold M, et al. Detection of early human papillomavirus-associated cancers by liquid biopsy. JCO Precis Oncol 2019;3:PO.18.00276.
18. Riaz N, Sherman E, Pei X, Schöder H, Grkovski M, Paudyal R, et al. Precision radiotherapy: reduction in radiation for oropharyngeal cancer in the 30 ROC trial. J Natl Cancer Inst 2021;113:742–51.
19. Lewis JS, Beadle B, Bishop JA, Chernock RD, Colasacco C, Lacchetti C, et al. Human papillomavirus testing in head and neck carcinomas: guideline from the College of American Pathologists. Arch Pathol Lab Med 2018;142:559–97.
20. Faden DL. Liquid biopsy for the diagnosis of HPV-associated head and neck cancer. Cancer Cytopathol 2021.
21. Rollo F, Dona' MG, Pellini R, Pichi B, Marandino F, Covello R, et al. Cytology and direct human papillomavirus testing on fine needle aspirates from cervical lymph node metastases of patients with oropharyngeal squamous cell carcinoma or occult primary. Cytopathology 2018;29:449–54.
22. Wong KS, Krane JF, Jo VY. Heterogeneity of p16 immunohistochemistry and increased sensitivity of RNA *in situ* hybridization in cytology specimens of HPV-related head and neck squamous cell carcinoma. Cancer Cytopathol 2019;127:632–42.
23. Xu B, Ghossein R, Lane J, Lin O, Katabi N. The utility of p16 immunostaining in fine needle aspiration in p16-positive head and neck squamous cell carcinoma. Hum Pathol 2016;54:193–200.
24. Yang Z, Gomez-Fernandez C, Lora Gonzalez M, Esebua M, Kerr DA. HPV testing through p16 immunocytochemistry in neck-mass FNA and its correlation with tissue samples. Cancer Cytopathol 2019;127:458–64.
25. Conrad R, Yang S-E, Chang S, Bhasin M, Sullivan PS, Moatamed NA, et al. Comparison of cytopathologist-performed ultrasound-guided fine-needle aspiration with cytopathologist-performed palpation-guided fine-needle aspiration: a single institutional experience. Arch Pathol Lab Med 2018;142:1260–7.
26. Chang Sing Pang KJW, Mur T, Collins L, Rao SR, Faden DL. Human papillomavirus in sinonasal squamous cell carcinoma: a systematic review and meta-analysis. Cancers 2020;13:45.
27. Chung CH, Zhang Q, Kong CS, Harris J, Fertig EJ, Harari PM, et al. p16 protein expression and human papillomavirus status as prognostic biomarkers of nonoropharyngeal head and neck squamous cell carcinoma. J Clin Oncol 2014;32:3930–8.
28. Mendez-Pena JE, Sadow PM, Nose V, Hoang MP. RNA chromogenic *in situ* hybridization assay with clinical automated platform is a sensitive method in detecting high-risk human papillomavirus in squamous cell carcinoma. Hum Pathol 2017;63:184–9.
29. Buch K, Fujita A, Li B, Kawashima Y, Qureshi MM, Sakai O. Using texture analysis to determine human papillomavirus status of oropharyngeal squamous cell carcinomas on CT. AJNR Am J Neuroradiol 2015;36:1343–8.
30. Fujita A, Buch K, Li B, Kawashima Y, Qureshi MM, Sakai O. Difference between HPV-positive and HPV-negative non-oropharyngeal head and neck cancer: texture analysis features on CT. J Comput Assist Tomogr 2016;40:43–7.
31. Fujita A, Buch K, Truong MT, Qureshi MM, Mercier G, Jalisi S, et al. Imaging characteristics of metastatic nodes and outcomes by HPV status in head and neck cancers. Laryngoscope 2016;126:392–8.
32. Fujima N, Andreu-Arasa VC, Meibom SK, Mercier GA, Truong MT, Sakai O. Prediction of the human papillomavirus status in patients with oropharyngeal squamous cell carcinoma by FDG-PET imaging dataset using deep learning analysis: a hypothesis-generating study. Eur J Radiol 2020;126:108936.
33. Onoue K, Fujima N, Andreu-Arasa VC, Setty BN, Qureshi MM, Sakai O. Cystic cervical lymph nodes of papillary thyroid carcinoma, tuberculosis and human papillomavirus positive oropharyngeal squamous cell carcinoma: comparative CT analysis for their differentiation. Eur J Radiol 2020;132:109310.

34. Onoue K, Fujima N, Andreu-Arasa VC, Setty BN, Sakai O. Cystic cervical lymph nodes of papillary thyroid carcinoma, tuberculosis and human papillomavirus positive oropharyngeal squamous cell carcinoma: utility of deep learning in their differentiation on CT. Am J Otolaryngol 2021;42:103026.
35. Chen F, Xue Y, Tan MT, Chen P. Efficient statistical tests to compare Youden index: accounting for contingency correlation. Stat Med 2015;34:1560–76.
36. Graboyes EM, Kompelli AR, Neskey DM, Brennan E, Nguyen S, Sterba KR, et al. Association of treatment delays with survival for patients with head and neck cancer: a systematic review. JAMA Otolaryngol Head Neck Surg 2019;145:166–77.
37. Saka-Herrán C, Jané-Salas E, Mari-Roig A, Estrugo-Devesa A, López-López J. Time-to-treatment in oral cancer: causes and implications for survival. Cancers 2021;13:1321.
38. Weller D, Vedsted P, Rubin G, Walter FM, Emery J, Scott S, et al. The Aarhus statement: improving design and reporting of studies on early cancer diagnosis. Br J Cancer 2012;106:1262–7.
39. Lee JY, Garcia-Murillas I, Cutts RJ, De Castro DG, Grove L, Hurley T, et al. Predicting response to radical (chemo)radiotherapy with circulating HPV DNA in locally advanced head and neck squamous carcinoma. Br J Cancer 2017;117:876–83.
40. Lewis JS, Mirabello L, Liu P, Wang X, Dupont WD, Plummer WD, et al. Oropharyngeal squamous cell carcinoma morphology and subtypes by human papillomavirus type and by 16 lineages and sublineages. Head Neck Pathol 2021;15:1089–98.
41. Gillison ML, Akagi K, Xiao W, Jiang B, Pickard RKL, Li J, et al. Human papillomavirus and the landscape of secondary genetic alterations in oral cancers. Genome Res 2019;29:1–17.
42. Mirabello L, Yeager M, Yu K, Clifford GM, Xiao Y, Zhu B, et al. HPV16 E7 genetic conservation is critical to carcinogenesis. Cell 2017;170:1164–74.
43. Rygalski CJ, Zhao S, Eskander A, Zhan KY, Mroz EA, Brock G, et al. Time to surgery and survival in head and neck cancer. Ann Surg Oncol 2021;28:877–85.